



Shock absorption of semi-interpenetrating network acrylic pressure-sensitive adhesive for mobile display impact resistance

Jong-Ho Back^{a,b}, Dooyoung Baek^{b,c}, Ji-Won Park^{b,c}, Hyun-Joong Kim^{b,c,*}, Joo-Young Jang^d, Seong-Ju Lee^d

^a Advanced Industrial Chemistry Research Center, Korea Research Institute of Chemical Technology (KRICT), Ulsan, 44412, Republic of Korea

^b Laboratory of Adhesion and Bio-Composites, Program in Environmental Materials Science, College of Agriculture and Life Sciences, Seoul National University, Seoul, 08826, Republic of Korea

^c Research Institute of Agriculture and Life Sciences, College of Agriculture and Life Sciences, Seoul National University, Seoul, 08826, Republic of Korea

^d ANYONE Inc, 6-45, 5th Cheonan Industrial Complex, Sushin-myeon, Dongnam-gu, Cheonan-si, Chungcheongnam-do, 31251, Republic of Korea

ARTICLE INFO

Keywords:

Adhesion
Pressure-sensitive adhesive
Impact
Semi-interpenetrating network
Mobile display

ABSTRACT

With the development of mobile display shapes from flat to flexible, the conventional glass cover window must be replaced by a film-type window. However, film-type cover windows have low impact resistance owing to their poor shock absorption. Therefore, to realize their application to flexible displays, it is essential to characterize and improve the shock-absorbing characteristics of the display film. In this study, a semi-interpenetrating network (semi-IPN) acrylic pressure-sensitive adhesive (PSA) consisting of a crosslinked network structure with a linear acrylic polymer chain was developed. The influence of the multi-functional monomer content and UV dose on the properties of the semi-IPN PSA was studied. The peel strength of the semi-IPN PSA was higher than 10 N/25 mm, which is generally considered as the PSA standard for mobile displays. With an increase in crosslink density, the storage modulus increased, but the damping factor decreased. To evaluate shock absorption, a falling ball impact tester was used to estimate the shock absorption ratio (ΔF) of the film. The semi-IPN PSA incorporating 30 phr of the multi-functional monomer exhibited higher ΔF (31.2%) than that of a conventional UV-curable PSA film (24.6%). This shows that even with the relatively low damping factor of the semi-IPN PSA, its structure could improve shock absorption. Moreover, we suggested two mechanisms for shock absorption of the semi-IPN PSA, energy dissipation into the PSA layer and extended contact time.

1. Introduction

Acrylic pressure-sensitive adhesives (PSAs) are used in various applications such as labeling as well as medical, packaging, and mobile phone applications, owing to their superior transparency and adhesion performance [1–7]. In mobile phones, acrylic PSAs are widely used for optically clear adhesive, back-glass tape, battery tape, light-shielding tape, shock-absorbing film, etc. The shock-absorbing film is located behind the organic light-emitting diodes (OLED) of the mobile phone to protect the OLED module, as shown in Fig. 1.

As mobile phone display changes from flat to flexible (e.g., curved,

foldable, and stretchable), its cover window should also change from conventional glass to film type. When a display experiences impact, a conventional glass cover window can absorb the impact energy by breaking itself; however, a film type cover window cannot do so. The diodes in a mobile phone are fragile and may be damaged if subjected to external impact. This scenario is even more likely when flexible displays are involved owing to the use of the film-type cover window. Therefore, for flexible display applications, it is important to characterize and improve the shock absorption properties of the display film.

By enhancing the shock absorption of both the shock-absorbing film and other PSA layers during assembly, the shock absorption of mobile

Abbreviations: Semi-IPN, semi-interpenetrating network; PSA, pressure-sensitive adhesive; OLED, organic light-emitting diodes; MFM, multi-functional monomer; TPGDA, tripropylene glycol diacrylate; GPC, gel permeation chromatography.

* Corresponding author. Lab. of Adhesion & Bio-Composites, Program in Environmental Materials Science, Seoul National University, Seoul, 08826, Republic of Korea.

E-mail address: hjokim@snu.ac.kr (H.-J. Kim).

URL: <http://www.adhesion.kr> (H.-J. Kim).

<https://doi.org/10.1016/j.ijadhadh.2020.102558>

Received 31 October 2019; Accepted 22 January 2020

Available online 6 February 2020

0143-7496/© 2020 Elsevier Ltd. All rights reserved.

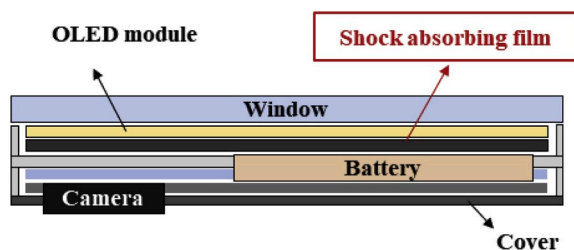


Fig. 1. Vertical structure of the mobile phone.

phones can be significantly improved. However, only a few studies focused on the shock absorption of PSAs. Although the effects of the strain rate on the mechanical properties of PSA have been studied [8–11], the mechanical properties of PSA under impact are still relatively unclear. Furthermore, there are several methods to quantitatively evaluate the impact resistance of thermosetting adhesives [12–17]. Particularly, the impact resistance of PSAs was estimated using drop impact tests of mobile phones [18,19], which is a qualitative rather than quantitative method and is unsuitable for a large number of tests due to the high cost of mobile phone module. In recent years, Hayashida et al. investigated the strain distributions of PSA during impact and quantitatively evaluated its impact resistance [20]; however, the authors only focused on the impact strength of the PSA, not its shock absorption characteristics.

To improve the shock absorption characteristics of PSA, the use of a semi-interpenetrating network (semi-IPN) may be considered. Semi-IPN is a structure consisting of a physically entangled crosslinked polymer network and linear polymer. Owing to the entangled structural effect of this network, a semi-IPN polymer has better damping properties than those of a simple crosslinked polymer [21]. In our research, we fabricated a semi-IPN acrylic PSA by adding a multi-functional monomer (MFM) into a linear acrylic PSAs, followed by UV polymerization [22–25] (Fig. 2). We successfully prepared the semi-IPN acrylic PSA and applied it to the chip packaging process of a semiconductor.

A falling ball impact tester was used to evaluate the shock absorption of the PSA under impact. The curing behavior, adhesion performance, and viscoelastic properties of the semi-IPN PSA were evaluated according to the UV dose, which is proportional to the degree of cross-linking. Moreover, its shock absorption was compared with that of a conventional UV-curable PSA film.

2. Experimental methods

2.1. Materials

The linear acrylic PSA consists of several acrylic monomers: 2-ethylhexyl acrylate (70 wt%), isobornyl acrylate (10 wt%), glycidyl methacrylate (10 wt%), and 2-hydroxyethyl acrylate (10 wt%), and was

synthesized by ethyl acetate as the solvent polymerization. Its basic properties are listed in Table 1. To incorporate the semi-IPN structure into the linear acrylic PSA, we used tripropylene glycol diacrylate (TPGDA, Miwon, Republic of Korea) as the MFM and 2-hydroxy-2-methylpropiophenone (Irgacure 1173, BASF, Germany) as the photo-initiator. Fig. 3 presents the chemical structure of the linear acrylic PSA and MFM. The reaction between the linear acrylic PSA and MFM is shown in Fig. 2.

2.2. Preparation of the semi-IPN PSA film

MFM was added to the linear acrylic PSA as 5, 10, 20, and 30 phr (per hundred resins, based on the solid weight of the linear acrylic PSA) and the photo-initiator was added as 3 wt% of the MFM content. These components were mixed by a paste mixer (ARE-310, Thinky, Japan) under 25 °C, 1700 rpm, and 5 min. After mixing, the mixture was coated on a film and then dried at 80 °C for 10 min. The dried PSA film was cured by UV irradiation (0, 100, 200, 400, 800, and 1200 mJ/cm²) and the PSA thickness was set to 60 μm.

2.3. Gel content

The gel content is the ratio of the crosslinked weight to the total weight. To measure the crosslinked weight of the cured film, we soaked the cured film in toluene for 24 h and filtered it using a 200-mesh filter. The gel content was calculated by Equation (1) as follows:

$$\text{Gel content [\%]} = \frac{W_{\text{mesh+soaked film}} - W_{\text{mesh}}}{W_{\text{film}}} \times 100. \quad (1)$$

where $W_{\text{mesh+soaked film}}$, W_{mesh} , and W_{film} are the weights of the mesh and soaked film, mesh, and film, respectively.

2.4. Adhesion performance

The semi-IPN PSA film was cut into 25-mm wide and attached to SUS 304 (stainless steel) substrate by a 2 kg rubber roller and stored at 23 °C for 24 h. The semi-IPN PSA film was detached at an angle of 180° with a constant crosshead rate of 300 mm/min using a texture analyzer (TA-TX plus, Micro Stable Systems, UK). The peel strength is the average force required to detach a PSA film from a substrate and is measured following

Table 1
Basic characteristics of the linear acrylic PSA.

Solid content [%]	Number average molecular weight, M_n^a [10^3 g/mol]	Weight average molecular weight, M_w^a [10^3 g/mol]	Dispersity, D^a
42.1 (±0.7)	46.5	723.4	15.6

^a Measured using gel permeation chromatography (GPC).

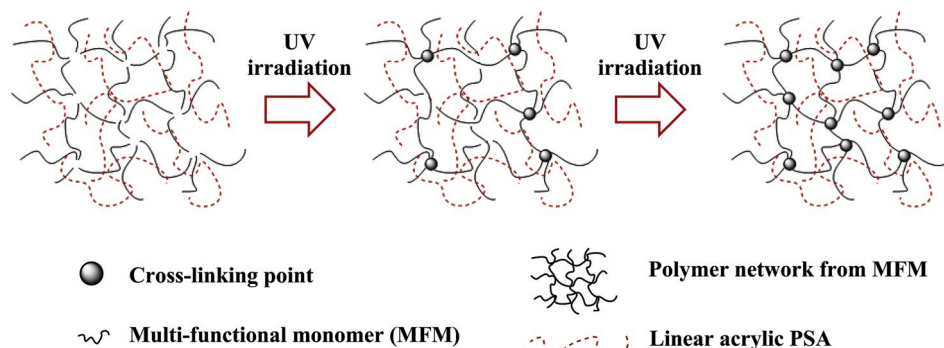


Fig. 2. Fabrication of semi-IPN PSA.

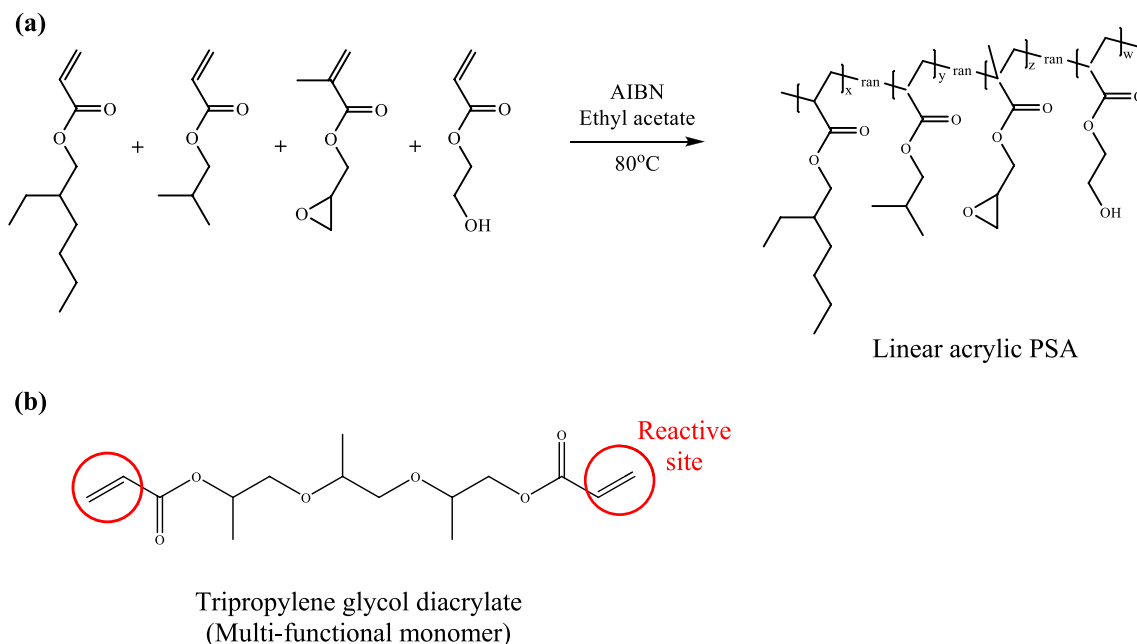


Fig. 3. Chemical structure of (a) linear acrylic PSA and (b) MFM.

ASTM D3330.

The probe tack quantifies the stickiness of the PSAs. To evaluate probe tack, we used a cylinder probe (substrate: SUS 304, diameter: 5 mm). The probe approached the semi-IPN PSA at 0.5 mm/s and contacted with it for 1 s while maintaining a constant applied force of 1 N. Afterward, the probe was separated from the semi-IPN PSA at 10 mm/s. The probe tack is the maximum force required to detach the probe from a PSA film and is tested following ASTM D2979. All measurements were repeated five times at a constant temperature of 25 °C.

2.5. Dynamic mechanical analysis

The viscoelastic property of the semi-IPN PSA was estimated by using dynamic mechanical analysis (DMA/SDTA, Mettler-Toledo Inc.,

Switzerland). The size of the specimen was 5 × 5×0.5 mm. A shear sandwich clamp was used and both temperature and frequency sweep were performed. For the temperature sweep, the temperature was increased at 5 °C/min from -40 °C to 80 °C with an amplitude of 16 μm and frequency of 1 Hz. For the frequency sweep, the frequency was increased from 0.1 to 100 Hz with an amplitude of 10 μm at 25 °C.

2.6. Impact tester

To quantitatively evaluate the shock absorption of the film under impact, we used a falling ball impact tester. We referred to ASTM D1709 (standard test methods for impact resistance of plastic film by free-falling dart method) and manually manufactured the falling ball impact tester for this study. The falling ball impact tester collects the

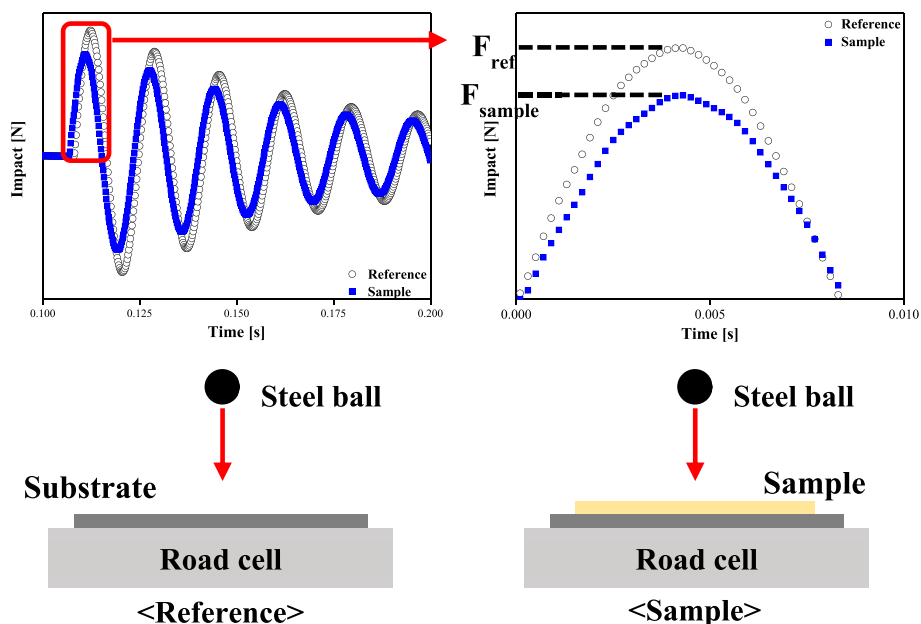


Fig. 4. Evaluation of shock absorption of the sample by using a falling ball impact tester.

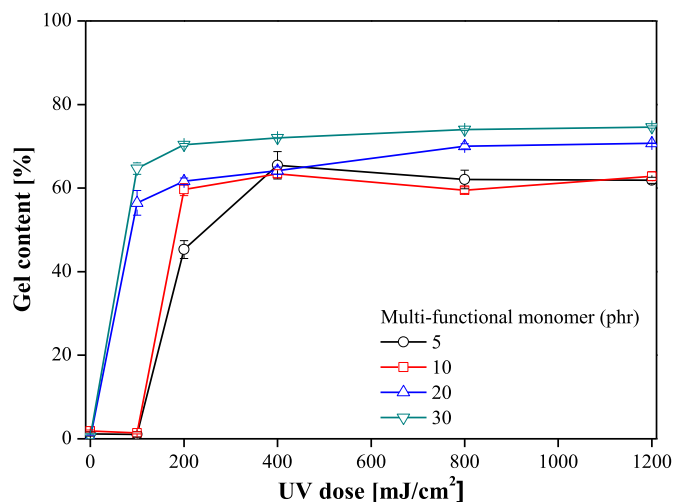


Fig. 5. Gel content of semi-IPN PSAs.

time-force data to evaluate the shock absorption of the PSA film rather than evaluate its impact resistance. A load cell of 1 kN was located at the bottom of the tester to quantitatively evaluate the force. The samples were attached to the steel substrate by constant force using a 2-kg roller as shown in Fig. 4 and a steel ball was dropped on the sample. The weight and height of the steel ball were adjusted to obtain an impact energy of 10 mJ. In the “Reference” state, no sample was placed on the load cell, whereas in the “Sample” state, a sample was placed on the load cell. As the sample partially absorbs the impact, there is a difference between the impact force of the “Reference” and “Sample” state. The shock absorption (ΔF) was evaluated by dividing the difference of the impact force ($F_{ref} - F_{sample}$) by the impact force of the “Reference” state (F_{ref}). All experiments were conducted at a constant temperature of 25 °C.

3. Results and discussion

3.1. Gel content

As shown in Fig. 5, the gel content increased up to 70% due to UV irradiation and MFM addition, which increased the portion of the crosslinked network. However, the weight fraction of the crosslinked network of the semi-IPN PSA should be less than 25 wt% because only MFM participated in the formation of the crosslinked network. This

indicates that the high level of gel content (70%) is caused by both the crosslinked network and linear polymer that are physically entangled with the network, thereby confirming the successful development of the semi-IPN structure.

3.2. Adhesion performance

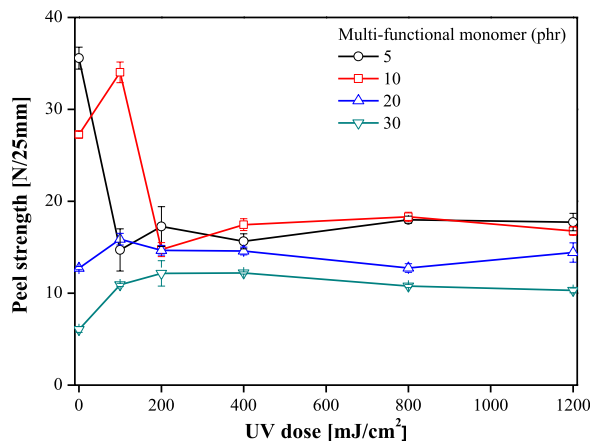
Fig. 6 shows the adhesion performance (peel strength and probe tack) of the semi-IPN PSA. Under 200 mJ/cm², the peel strength and probe tack were roughly improved by UV irradiation because of the better cohesion strength from crosslinking (except for the peel strength of 5 phr of MFM). At high UV dose, the peel strength and probe tack decreased because of the deteriorated wetting property due to the highly dense crosslinked network. As the MFM content was increased, the peel strength and probe tack decreased because of the dense crosslinked network. All samples have peel strengths higher than 10 N/25 mm, which is generally regarded as the minimum standard value of the adhesion strength in a mobile display application. This indicates that all prepared semi-IPN PSA could be applied to the mobile display considering their adhesion performances.

3.3. Viscoelastic property

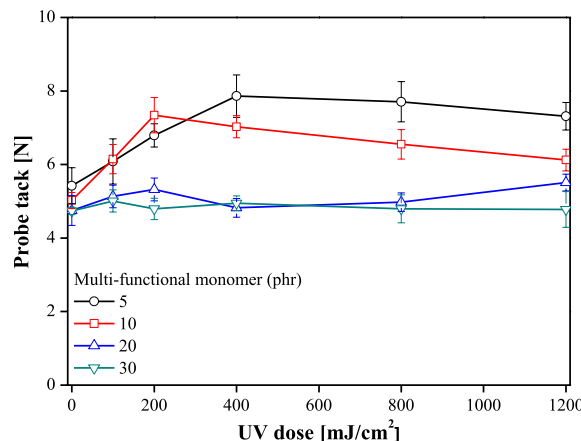
The storage modulus and damping factor ($\tan \delta$) were estimated under temperature and frequency sweep conditions, respectively (Fig. 7). The storage modulus of the semi-IPN PSA for both temperature and frequency sweep conditions was enhanced with the increase of MFM content resulting in high crosslink density. As the MFM content was increased, the semi-IPN PSA became rigid due to high crosslink density, thereby decreasing the peak height of $\tan \delta$. At 30 phr of MFM, phase separation occurred for $\tan \delta$ at 0 and 60 °C (Fig. 7 (b)). The two peaks of $\tan \delta$ at low (0 °C) and high (60 °C) temperatures corresponded to the glass transition temperature for linear and crosslinked polymer, respectively. This demonstrated the successful development of the semi-IPN structure involving a physically but not chemically entangled linear and crosslinked polymer.

3.4. Shock absorption

The shock absorption of the semi-IPN PSA was evaluated using the falling ball impact tester (Fig. 8). It was compared with the shock absorption of a simple-crosslinked conventional PSA by UV irradiation (ANYONE Inc.) that had similar composition with the developed linear acrylic PSA. As the UV dose was increased, the conventional PSA was randomly crosslinked to increase rigidity. When the steel ball was



(a)



(b)

Fig. 6. (a) Peel strength and (b) probe tack of the semi-IPN PSA.

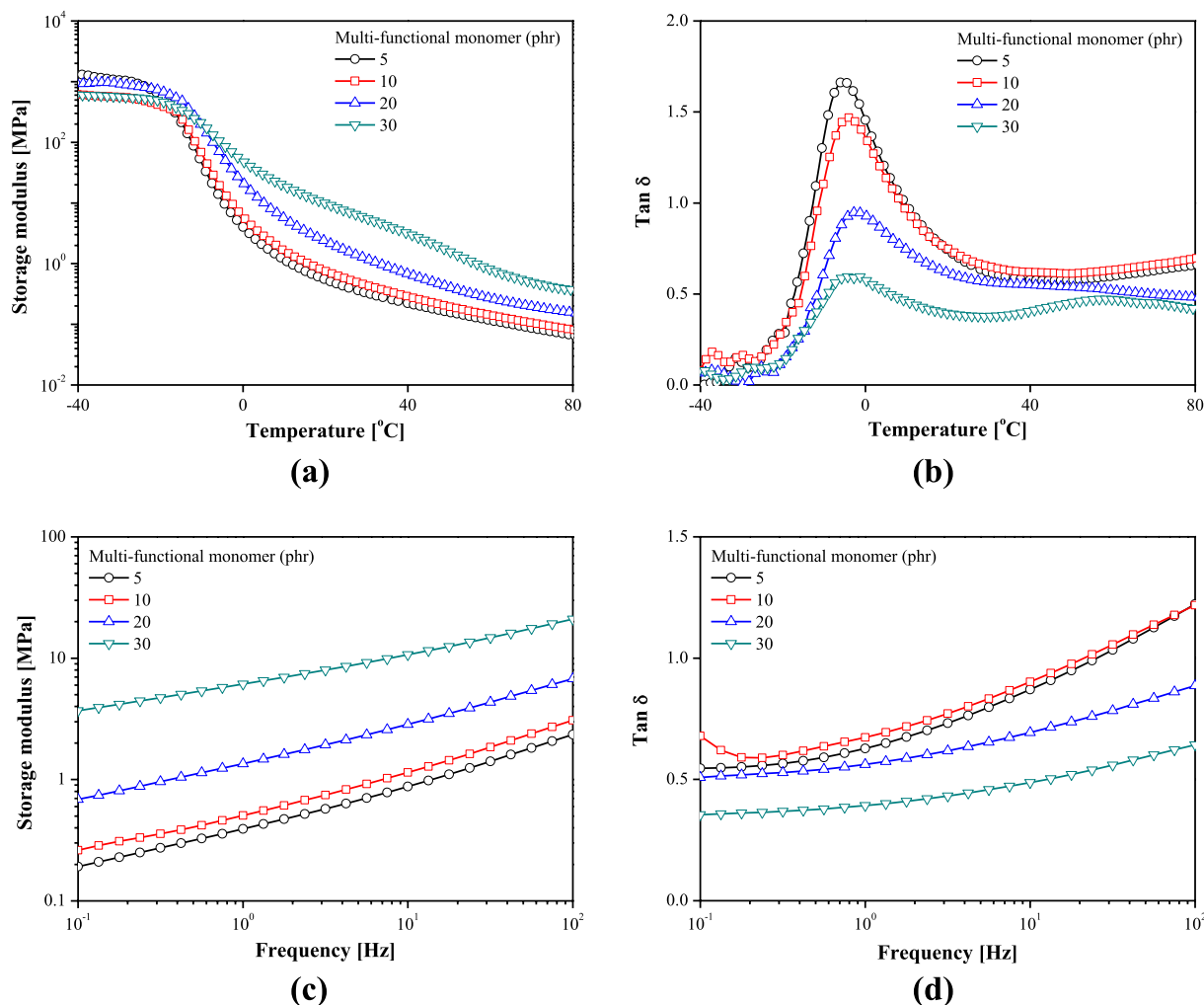


Figure 7. (a, c) Storage modulus and (b, d) tan δ of the semi-IPN PSA cured by 1200 mJ/cm² UV by temperature sweep and frequency sweep mode, respectively.

dropped on the PSA, the kinetic energy of the steel ball was transferred to the PSA. Although the momentum area in the force-time curve was similar, the impact force representing the maximum force in the force-time curve changed according to the PSA rigidity. Hence, despite a similar momentum, increased rigidity of the PSA increased the impact force owing to the reduced contact time. This indicates that the high

crosslink density of the conventional PSA resulted in a low shock absorption capacity (Fig. 8). Likewise, for semi-IPN PSA, the shock absorption was initially decreased according to the increased UV dose with increased crosslink density (Fig. 8). However, unlike the steady downward curve of the conventional PSA, the shock absorption of the semi-IPN PSA increased slightly at high UV dose and high MFM content. At the maximum UV dose, the ΔF value of the semi-IPN PSA was much higher (31.2%) than that of the conventional PSA (15.9%), thereby demonstrating the effect of the semi-IPN structure on shock absorption.

As shown in Fig. 9, when the steel ball was dropped on the semi-IPN PSA, the kinetic energy of the steel ball was transferred to the PSA layer. The impact force from the transferred energy could be absorbed into the PSA layer by two mechanisms. Firstly, during the contact between the steel ball and PSA, the maximum impact force could be reduced with extended contact time. If the impact energy (area under the time-force curve) is constant, the maximum impact force should be reduced when the contact time increased. In the case of the semi-IPN PSA, extending the contact time might occur from the entanglement of the linear polymer with the crosslinked network. Secondly, the transferred energy from the steel ball could be dissipated into the semi-IPN PSA layer to reduce the maximum impact force. The semi-IPN PSA included a crosslinked network structure effective for the dissipation of transferred energy. These two mechanisms for shock absorption occurred simultaneously for the semi-IPN PSA, thus resulting in its superior shock absorption compared to that of other films.

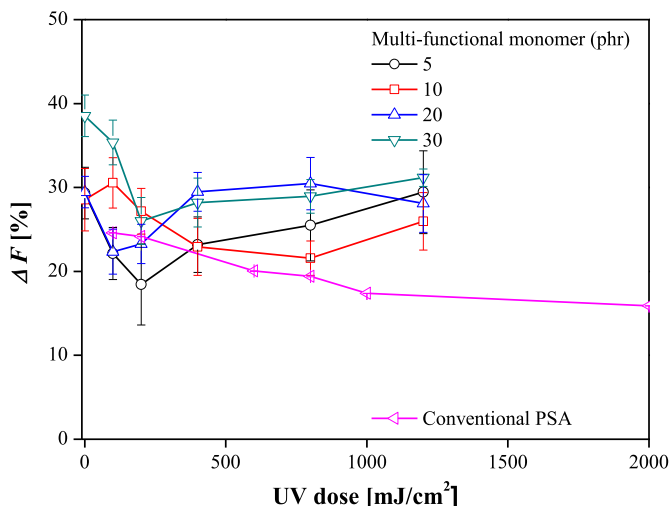


Fig. 8. Shock absorption of the semi-IPN PSA and conventional PSA.

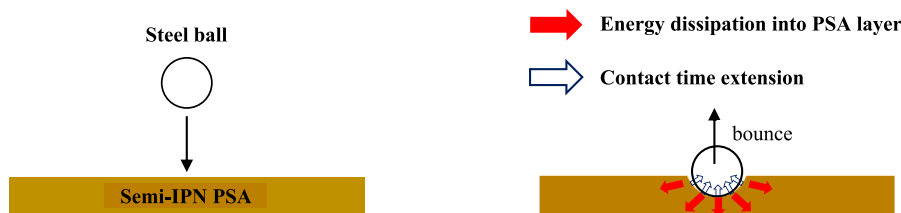


Fig. 9. Schematic for shock absorption of the semi-IPN PSA.

4. Conclusions

Appropriate shock absorption capacities could prevent damaging a mobile phone when subjected to external impact, thereby extending the service life of a mobile phone. To improve the shock absorption of a mobile phone, we developed a semi-IPN PSA and evaluated its basic properties including the gel content, adhesion performance, viscoelastic properties, and shock absorption. The developed semi-IPN PSA demonstrated satisfactory gel content and adhesion performance confirmed by the phase separation of $\tan \delta$. We used a falling ball impact tester to estimate the shock absorption ratio (ΔF) of the semi-IPN PSA. At maximum UV dose, the ΔF value of the semi-IPN PSA was much higher (31.2%) than that of the conventional PSA (15.9%). Furthermore, 30-phr MFM content was the best composition to achieve high shock absorption. The superior shock absorption of semi-IPN PSA can be attributed to two simultaneously occurring mechanisms: energy dissipation into the PSA layer and extended contact time. The semi-IPN PSA developed in this study demonstrated better shock absorption than other films. However, we only focused on the maximum force to calculate the shock absorption of the PSA. The shock absorption mechanism is still unclear. Therefore, future work must focus on investigating both impact force and contact time to specifically establish the shock absorption mechanism.

Acknowledgements

This work was supported by Anyone Inc., Republic of Korea.

References

- [1] Schlademan J. Handbook of pressure sensitive adhesive technology. New York: Satas Donatas; 1989.
- [2] Czech Z, Kurzawa R. Acrylic pressure-sensitive adhesive for transdermal drug delivery systems. *J Appl Polym Sci* 2007;106:2398–404.
- [3] Lee SW, Lee TH, Park JW, Kim HJ. Synthesis and UV-curing behaviors of urethane acrylic oligomers modified by the incorporation of silicone diols into the soft segments for a 3D multi-chip package process. *J Electron Mater* 2015;44:2406–13.
- [4] Lee JH, Lee TH, Shim KS, Park JW, Kim HJ, Kim Y, et al. Molecular weight and crosslinking on the adhesion performance and flexibility of acrylic PSAs. *J Adhes Sci Technol* 2016;30:2316–28.
- [5] Lee JH, Lee TH, Shim KS, Park JW, Kim HJ, Kim Y, et al. Effect of crosslinking density on adhesion performance and flexibility properties of acrylic pressure sensitive adhesives for flexible display applications. *Int J Adhesion Adhes* 2017;74: 137–43.
- [6] Park CH, Lee SJ, Lee TH, Kim HJ. Characterization of an acrylic polymer under hygrothermal aging as an optically clear adhesive for touch screen panels. *Int J Adhesion Adhes* 2015;63:137–44.
- [7] Park CH, Lee SJ, Lee TH, Kim HJ. Characterization of an acrylic pressure-sensitive adhesive blended with hydrophilic monomer exposed to hygrothermal aging: assigning cloud point resistance as an optically clear adhesive for a touch screen panel. *React Funct Polym* 2016;100:130–41.
- [8] Gibert F, Allal A, Marin G, Deraill C. Effect of the rheological properties of industrial hot-melt and pressure-sensitive adhesives on the peel behavior. *J Adhes Sci Technol* 1999;13:1029–44.
- [9] Marin G, Deraill C. Rheology and adherence of pressure-sensitive adhesives. *J Adhes* 2006;82:469–85.
- [10] Du J, Lindeman D, Yarusso D. Modeling the peel performance of pressure-sensitive adhesives. *J Adhes* 2004;80:601–12.
- [11] Urahama Y. Effect of peel load on stringiness phenomena and peel speed of pressure-sensitive adhesive tape. *J Adhes* 1989;31:47–58.
- [12] Goglio L, Rossetto M. Impact rupture of structural adhesive joints under different stress combinations. *Int J Impact Eng* 2008;35:635–43.
- [13] Kadioglu F, Adams RD. Flexible adhesives for automotive application under impact loading. *Int J Adhesion Adhes* 2015;56:73–8.
- [14] Neumayer J, Kuhn P, Koerber H, Hinterhölzl R. Experimental determination of the tensile and shear behaviour of adhesives under impact loading. *J Adhes* 2016;92: 503–16.
- [15] Adachi T, Kataoka T, Higuchi M. Predicting impact shear strength of phenolic resin adhesive blended with nitrile rubber. *Int J Adhesion Adhes* 2015;56:53–60.
- [16] Hazimeh R, Challita G, Khalil K, Othman R. Finite element analysis of adhesively bonded composite joints subjected to impact loadings. *Int J Adhesion Adhes* 2015; 56:24–31.
- [17] Machado J, Marques E, da Silva LF. Adhesives and adhesive joints under impact loadings: an overview. *J Adhes* 2017:1–32.
- [18] Hwan CL, Lin MJ, Lo CC, Chen WL. Drop tests and impact simulation for cell phones. *J Chin Inst Eng* 2011;34:337–46.
- [19] Karppinen J, Li J, Pakarinen J, Mattila TT, Paulasto-Kröckel M. Shock impact reliability characterization of a handheld product in accelerated tests and use environment. *Microelectron Reliab* 2012;52:190–8.
- [20] Hayashida S, Sugaya T, Kuramoto S, Sato C, Mihara A, Onuma T. Impact strength of joints bonded with high-strength pressure-sensitive adhesive. *Int J Adhesion Adhes* 2015;56:61–72.
- [21] Suresh K, Vishwanatham S, Bartsch E. Viscoelastic and damping characteristics of poly (n-butyl acrylate)-poly (n-butyl methacrylate) semi-IPN latex films. *Polym Adv Technol* 2007;18:364–72.
- [22] Joo HS, Do HS, Park YJ, Kim HJ. Adhesion performance of UV-cured semi-IPN structure acrylic pressure sensitive adhesives. *J Adhes Sci Technol* 2006;20: 1573–94.
- [23] Joo HS, Park YJ, Do HS, Kim HJ, Song SY, Choi KY. The curing performance of UV-curable semi-interpenetrating polymer network structured acrylic pressure-sensitive adhesives. *J Adhes Sci Technol* 2007;21:575–88.
- [24] Lee SW, Park JW, Kim HJ, Kim KM, Kim HI, Ryu JM. Adhesion performance and microscope morphology of UV-curable semi-interpenetrated dicing acrylic PSAs in Si-wafer manufacture process for MCP. *J Adhes Sci Technol* 2012;26:317–29.
- [25] Lee SW, Park JW, Kwon YE, Kim S, Kim HJ, Kim EA, et al. Optical properties and UV-curing behaviors of optically clear semi-interpenetrated structured acrylic pressure sensitive adhesives. *Int J Adhesion Adhes* 2012;38:5–10.